Analytica Chimica Acta 1198 (2022) 339531

Contents lists available at ScienceDirect

Analytica Chimica Acta

journal homepage: www.elsevier.com/locate/aca

Construction of anthraquinone functional zinc phthalocyanine sensor platform for ultra-trace amount of water determination in tetrahydrofuran and *N*,*N*-Dimethylformamide

Mustafa Semih Yildirim [a], Yusuf Alcay [a], Ozgur Yavuz [a], Secil Kirlangic Atasen [b], Zeliha Mermer [a], Hulya Aribuga [a], Ismail Yilmaz [a, *]

[a] Istanbul Technical University, Department of Chemistry, 34469, Maslak, Istanbul, Turkey
[b] Istanbul Gelisim University, Laboratory Technology Department, Vocational School of Health Services, Avcilar, Istanbul, Turkey

HIGHLIGHTS

- Anthraquinone functional zinc phthalocyanine sensor was utilized for ultra-trace amount of water detection in organic solvents.
- The Sensor was used for water sensing through voltammetric and fluorometric methods with detailed mechanistic explanations.
- The sensor displays very low LOD value and fast response time, and has high stability during experiments.

GRAPHICAL ABSTRACT

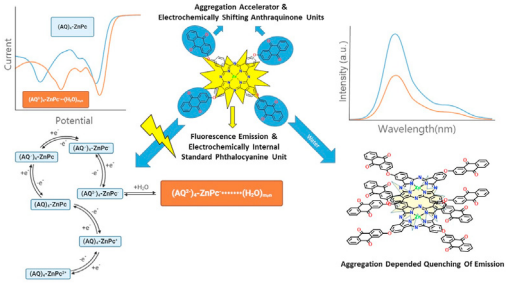

ARTICLE INFO

Article history:
Received 18 July 2021
Received in revised form
11 December 2021
Accepted 18 January 2022
Available online 20 January 2022

Keywords:
Water sensor
Phthalocyanine
Anthraquinone
Fluorescence
Electrochemistry

ABSTRACT

Anthraquinone functional zinc phthalocyanine sensor platform was utilized for ultra-trace amount of water determination in THF and DMF. Using the fluorometric method, the water content in THF was determined with a LOD of 2.27×10^{-4} M and a response time of 1 s. The sensor is based on the mechanism of aggregation depended on quenching of emission. Although the aggregation is known as an undesirable property in the application of phthalocyanine, this property has been successfully applied in the quantification of water content in THF. By using the shift of the third reduction wave of the sensor, the water content in DMF was measured with a LOD value of 5.64×10^{-7} M. The voltammetric response mechanism is based on the hydrogen bonding depended shifting of the reduction potential of quinone moiety on phthalocyanine. Redox potentials of phthalocyanine are used as a calibrant for accurate quantification of water content in DMF. Water molecules (n and m) and equilibrium constants (K^1 and K^2) for the formation of hydrogen bonding for the first and third reduction processes were calculated as 1.18 (n), 10.4 (m) and 19.3 (K^1), 1.6×10^{11} (K^2) $M^{-(m-n)}$, which demonstrated why the third reduction process was chosen to set the calibration plots.

1. Introduction

Water is considered a significant impurity and contaminant for many organic solvents. Determination and measurement of trace

* Corresponding author.
E-mail address: iyilmaz@itu.edu.tr (I. Yilmaz).

https://doi.org/10.1016/j.aca.2022.339531
0003-2670/

amount of water are vital for environmental monitoring, food processing, pharmaceutical, biomedical, and petroleum-based fuels [1,2]. Karl Fischer is a well-known method for determining the water content in organic solvents. Although the method has the capability of low detection limit, it brings along some disadvantages; the usage of toxic chemicals (i.e., imidazole, I_2, and SO_2), needing a long measurement time, and interference from other typical coexisting species [3]. The sensing instruments for water determination can be varied, and there are many examples in literature, such as holographic sensors, optical changes-based sensors, polymer-coated platinum electrode sensors, and IR water sensors [4–7]. With the advancement of optical innovation, the fluorescent sensors turn into a very attractive subject in a broad scope owing to their high sensitivity and selectivity, advantageous activity, fast response, and low cost. For the water detection in the organic solvents, some organic fluorescence molecules have been developed in recent years. In this manner, the construction of new fluorescence probes for water quantification in organic solvents continues to be an interesting subject for researches [8–10].

Phthalocyanine (Pc) molecules have unique spectral and electrochemical characteristics due to their macrocyclic, deep conjugated molecular structure. After first synthesized in the early 20th century, it has been found that there are a lot of applications such as sensors, photodynamic therapy agents, catalysts, and organic semiconductors. Moreover, chemical modifications of peripheral/non-peripheral position and changing of the central metal atom in the Pc center give many different types of Pc complexes with various features, permitting the fine-tuning of intended physicochemical characteristics [11–17]. With the effect of aggregation, Pc molecules become very sensitive against polar solvents especially aqueous solvents. Metallophthalocyanines (MPc), especially with miscellaneous groups at the peripheral position of Pc core which expands π electrons in the planar macrocycle ring, tend to highly aggregate in solution, resulting in diminishing the fluorescence quantum yield and photosensitizing ability [18,19]. Although the aggregation properties of Pc molecules and their negative effects in many applications are well-known in the literature [20,21], the applicability of this property such as water determination in solvents has not been evaluated. On the other hand, Pc molecules exhibit very rich redox chemistry which is very effectively utilized in many electrochemical applications such as electrocatalyst [22,23] and electrochemical sensors [11,24,25]. However, until now, the electrochemistry of Pc molecules has never been used in water determination in organic solvents. Similar to Pc, quinones, another important class of compounds, also exhibit rich electrochemical behavior due to their carbonyl functional groups [26,27] which can be reversibly reduced to mono-anionic and di-anionic species in organic solvents. In our previous study, the quinone derivatives carrying ferrocene unit enabled us to determine the water content in organic solvents by creating hydrogen bonds with the reduced oxygen atoms of quinone and water molecules [28]. In this study, we focused on quantification of water content in organic solvents (THF and DMF) using a chemosensor based on the mechanism of aggregation depended on quenching of emission (ADQE) for fluorometric method, and hydrogen bonding depended shifting of the reduction potential of quinone moiety on the Pc molecules for voltammetry. To realize this objective, we utilized the Pc molecule **$(AQ)_4$-ZnPc** containing Pc skeleton and anthraquinone **(AQ)** moieties with a highly planar structure and deeper π electron conjugation, leading to high aggregation and rich electrochemistry. Although there are some dual-channel water sensors based on optical methods such as absorption and fluorescence methods [9,10,29,30] **$(AQ)_4$-ZnPc** is the first sensor used for water detection based on fluorometric and voltammetric methods. Kim et al. were published a very useful and comprehensive review about sensors for water recognition in organic solvents based on various mechanisms such as aggregation-induced emission (AIE), intramolecular charge transfer (ICT), excited-state intramolecular proton transfer (ESIPT), aggregation based monomer–excimer/exciplex switching, water-induced interpolymer π-stacking aggregation with comparing the sensor capability of the different studied probes [31]. Among all of these sensing mechanisms, **$(AQ)_4$-ZnPc** has a distinct sensing platform based on the ADQE mechanism. Although Pc molecules were effectively used in sensor applications owing to their high stability, rich photochemical properties, and long-wavelength emissions, **$(AQ)_4$-ZnPc** was utilized for the first time as a Pc-based sensor to determine the trace amount of water in organic solvents. In this study, the purpose of the AQ is to utilize its electroactive properties for electrochemical analysis of trace amount of water in DMF by using the shift of the second reduction wave of the AQ units in the Pc. This shift is due to the formation of the hydrogen binding between the dianionic species of AQ and water molecules. On the other hand, the reason of using AQ moiety is to extend flatness like structure of the phthalocyanine to increase the intensity of aggregation for spectroscopic analysis. The square wave voltammetric (SWV) method was successfully applied for a trace amount of water detection in DMF, where the second electro-reduced species of anthraquinone units and the first electro-oxidized/second electro-reduced Pc of sensor **$(AQ)_4$-ZnPc** were used as water receptor and internal standard, respectively. The new sensor **$(AQ)_4$-ZnPc** with improved analytical performances is one of the most favorable sensors used for a trace amount of water detection in THF and DMF.

2. Experimental section

2.1. Chemicals

DBU (1,8-diazabicyclo[5.4.0]undec-7-ene), dimethyl sulfoxide (DMSO), phthalimide, anhydrous zinc acetate, 2-hydroxyanthraquinone, 1-hexanol, methanol (MeOH), ethanol (EtOH), molecular sieves (3 Å), silica gel, dichloromethane (DCM), tetrahydrofuran (THF), hexane, diethyl ether (Et_2O), benzene, toluene, 1,4-dioxane, acetone, dimethylformamide (DMF), and acetonitrile (ACN) were purchased from commercial suppliers. Starting from phthalimide, 4-nitrophthalonitrile **(1)** was prepared in three-step according to the known procedure [32]. Anthraquinone substituted phthalonitrile **(2)** was obtained using 2-hydroxyanthraquinone and **(1)** in the presence of Na_2CO_3 under argon atmosphere at 45 °C considering the procedure of a nucleophilic aromatic substitution reaction [33]. Synthesizing of tetra anthraquinone zinc phthalocyanine **$(AQ)_4$-ZnPc** was conducted with zinc acetate and **(2)** with DBU base under argon atmosphere at 160 °C according to literature method [34].

2.2. Apparatus

The UV–Vis studies were performed by Agilent 8453 spectrophotometer with 1 cm path length cuvettes at 25 °C. The fluorescence studies were carried out by a Varian Cary Eclipse fluorophotometer (λ_{ex} = 605 nm). Square Wave Voltammetry (SWV) and Cyclic Voltammetry (CV) were studied by Princeton Applied Research Model 2263 potentiostat with a computer. A three-electrode system with a solid cell stand was utilized for SWV and CV measurements in DMF, where glassy carbon (GC) (3.0 mm diameter) disc, a platinum wire (PW), and Ag/AgCl were used as working, counter, and reference electrodes. By using high purity argon, the presence of oxygen was removed from the solution of **$(AQ)_4$-ZnPc** before starting the experiment. The solution of **$(AQ)_4$-ZnPc** was maintained from the air by the argon atmosphere during

the measurements. The solid electrodes were polished on alumina (<10 μM) slurries on BAS feltpad, and then rinsed with distilled water and then EtOH.

2.3. Measurement procedure

To get ultra-dried solvent, the purchased electrochemical gradient THF was distilled over sodium-benzophenone drying system, and held in a cell that contains fresh 3 Å molecular sieve which was regenerated in an oven at 573 K, and allowed to cool for three days under an argon atmosphere in the glass apparatus [28,35]. Using this method, we were able to obtain ultra-dry THF containing about only 0.8 ppm water (measured by Karl-Fisher). For fluorometric titration experiments, 3.5 mg of **$(AQ)_4$-ZnPc** was dissolved in THF (10.0 mL), and used as stock solution. Afterward, a titration experiment was performed at 9.0×10^{-6} M concentration of **$(AQ)_4$-ZnPc**. This concentration was chosen according to the linear calibration curve of the probe in aggregation studies based on the relation between concentration to fluorescence intensity (Fig.S1). Every titration and aggregation measurements were performed in a freshly prepared **$(AQ)_4$-ZnPc** solution to prevent the solution from moisture. The titrations were performed in 7.0 ml (1.0 cm diameter) of the test tube by adding water via microliter syringe with installing over septum. Moreover, utilizing this simple closed system, either diffusing of moisture from the air into the solution could be prevented, or successfully measurements without the need for a system that is not always available, such as glovebox were performed during the measurements time (the water content was always controlled by Karl-Fisher during experiments).

The purchased electrochemical grade DMF was dried with a 3 Å molecular sieve in a glass container under a vacuum desiccator for 4 days. For analysis, similar to fluorometric titration, water was added by microliter syringe sequentially into the electrochemical cell containing 2.0×10^{-3} M probe. The spectrophotometric and voltammetric titration experiments have been done for 3 times.

2.4. Fluorescence quantum yield of (AQ)4-ZnPc

The fluorescence quantum yield ($\mathbf{\Phi_F}$) can be shortly explained as the ratio of the number of photons emitted by the fluorescence molecule to the number of photons absorbed by the molecule. In this study, to calculate the $\boldsymbol{\Phi_F}$ of **$(AQ)_4$-ZnPc** fluorophore molecule via Williams's equation, non-substituted ZnPc was chosen as a reference because of its similar absorption and emission characteristics with the probe molecule [36]. After carrying out all necessary absorption and emission reading in THF, we calculated the quantum yield of **$(AQ)_4$-ZnPc** as 0.18. It is worth mentioning here, unless ultra-dried THF is used in the studies, the $\boldsymbol{\Phi_F}$ has dramatically decreased because of polarity dependent-aggregation of Pc compounds.

3. Result and discussion

3.1. Spectral properties and response mechanisms

The UV–Vis spectrum of **$(AQ)_4$-ZnPc** exhibits characteristic Soret (B-band) at 349 nm and Q-band with more intense at 673 nm (Fig.S2a). The fluorescence spectrum of **$(AQ)_4$-ZnPc** displayed an intense emission band at 683 nm when excited at 605 nm (Fig.S2b). These bands are well-known properties of Pc molecules having deep 18-π electron conjugation system, leading to the strong π-π* electronic transitions.

Aggregation behavior of Pc is delineated as a coplanar union of the Pc rings, which is a result of changing from mono form of the macrocyclic ring to dimer and higher order. It is mainly interested with type of solvent, substituents, and metal cations as well concentration and temperature [37,38]. It is a common knowledge that the absorption and emission wavelengths are very sensitive to the environmental factors like solvent polarity [39]. Moreover, in the presence of polar or aqueous solvents, the aggregation band in the absorption spectrum of Pc becomes very obvious at just the left side of Q-band [40]. Thus, the absorption spectrum of **$(AQ)_4$-ZnPc** is consistent with this solvent polarity effect and solubility in the context of aggregation in THF, 1,4-dioxane, DMSO, and DMF solvents in Fig. 1. The aggregation band of **$(AQ)_4$-ZnPc** in DMSO is higher than its Q-band absorption due to the face-to-face stacking of the Pc molecules. Exceptionally, although the same strong aggregation behavior of **$(AQ)_4$-ZnPc** is expected for DMF solvent, its aggregation is lower than even 1,4-dioxane because DMF can be axially coordinated by Zn metal center, preventing the π-π stacking of the Pc molecules and better solubility in DMF [41]. Moreover, THF has the highest main Q-band absorption band due to its low polarity and good solubility. However, the differences observed in the aggregation of **$(AQ)_4$-ZnPc** in the solvents are also probably due to a combination of coordination ability of the solvent, solvent polarity, and solubility of the compound. To observe the aggregation effect of water on **$(AQ)_4$-ZnPc** in THF, the UV–Vis spectra of **$(AQ)_4$-ZnPc** were recorded by changing the amount of water in THF. It can be obviously seen from Fig. 2 that the increases in the absorbance of the aggregation band of **$(AQ)_4$-ZnPc** are proportional to the amount of water in THF. Moreover, when adding other organic solvents/contaminants such as ACN, furan, phenol, aniline, and alcohol as like 15% to total amount of THF solution of the **$(AQ)_4$-ZnPc**, same polarity and π - π stacking induced aggregation of Pc resulted in UV–Vis spectrum (Fig. S3). Interestingly, aniline has caused to red shift of Q-band of the **$(AQ)_4$-ZnPc** while the phenol has no significant change in wavelength of Q-band. The probable reason may be the basicity of aniline. MeOH and ACN are two solvents that are drastically decreased Q-band of the **$(AQ)_4$-ZnPc** while, water has caused mostly increased aggregation band of the **$(AQ)_4$-ZnPc**.

The UV–Vis spectra of **$(AQ)_4$-ZnPc** without water and with 15% water in THF (inset in Fig. 2) show isosbestic points at 657 nm and 684 nm, indicating formation of aggregated products. The UV–Vis spectra of **$(AQ)_4$-ZnPc** in THF with 0–0.245 M water were also measured to understand UV–Vis sensitivity performance of the probe. As seen from Fig. S4, the Q-band of the probe is slightly decreased in THF with 0–0.245 M water. However, our analytical studies were realized using highly sensitive fluorescence spectroscopy as discussed below. To further prove the aggregation dependence of the quenching mechanism of the probe, MALDI-TOF mass analysis in dry THF and THF containing 15% water was performed. Fig. 3a shows the peak corresponding to only monomeric **$(AQ)_4$-ZnPc3H$^+$** probe molecule in dry THF. However, Fig. 3b illustrates the mass results that accordance with the calculated mass value of the monomeric, dimeric, and trimeric structures of the **$(AQ)_4$-ZnPcH$^+$** which were formed due to the aggregation of **$(AQ)_4$-ZnPc** molecules.

We also carried out an experiment that demonstrated the temperature effect on fluorescence emission (Fig. S5). As a result of gradual increased temperature, the fluorescence intensity started to elevate, which might be resulted from preventing aggregate dimer or higher order Pc complexes thanks to the temperature effect.

3.2. Spectral changes in different solvents

Aggregation effects of various solvents on **$(AQ)_4$-ZnPc** in THF were monitored by the fluorescence intensity changes (Figs. 4 and S6). The graphs are extracted from adding 20.0 μL different solvents

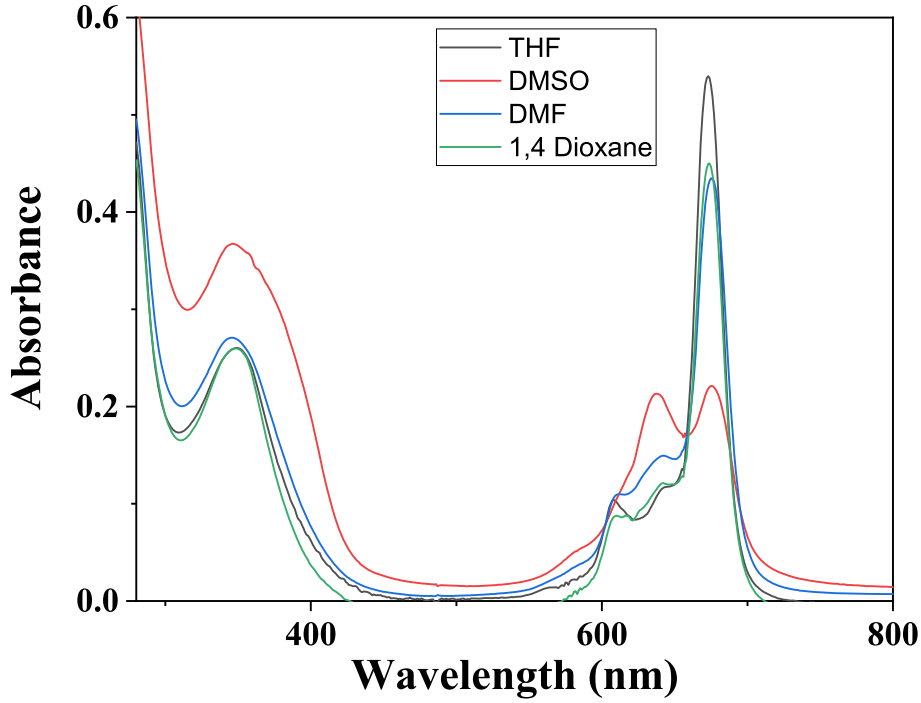

Fig. 1. The UV–Vis spectra of **$(AQ)_4$-ZnPc** in dried DMSO, DMF, 1,4-dioxane, and THF. [**$(AQ)_4$-ZnPc**] = 9.0×10^{-6} M.

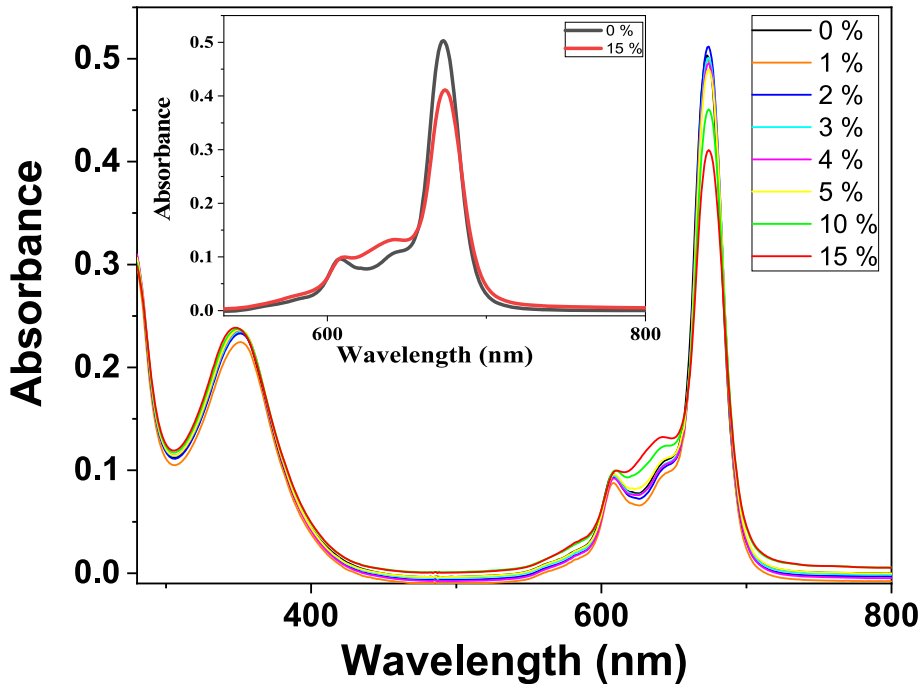

Fig. 2. The UV–Vis spectra of **$(AQ)_4$-ZnPc** recorded by changing the amount of water in THF. Inset: The UV–Vis spectra of **$(AQ)_4$-ZnPc** without water and with 15% water in THF. [**$(AQ)_4$-ZnPc**] = 9.0×10^{-6} M. The UV–Vis spectra were taken after waiting for more than 1 min for each measurement to attain an equilibrium.

into the 7.0 mL **$(AQ)_4$-ZnPc** solution in THF that was freshly prepared for each experiment (Fig. 4). Considering the quench effect of solvents, it is easily understood that the solvent polarity causes the aggregation of the Pc molecule. MeOH, DMF, DMSO, and water cause to decrease dramatically fluorescence intensity. This property of Pc molecules is well-known literature information [42]. As seen from Fig. 4, the most prominent aggregation effect was observed for water as expected. However, when benzene and toluene solvents are taken into account, the polarity effect is not enough to explain the quenching, which it can be elucidated considering the molecular structure of solvents. While benzene has a planar structure, toluene has one sp^3 hybrid methyl group that deviates flatness of the Pc molecule. Moreover, the planar benzene facilitates the π–π stacking of the Pc molecules which impels to aggregation

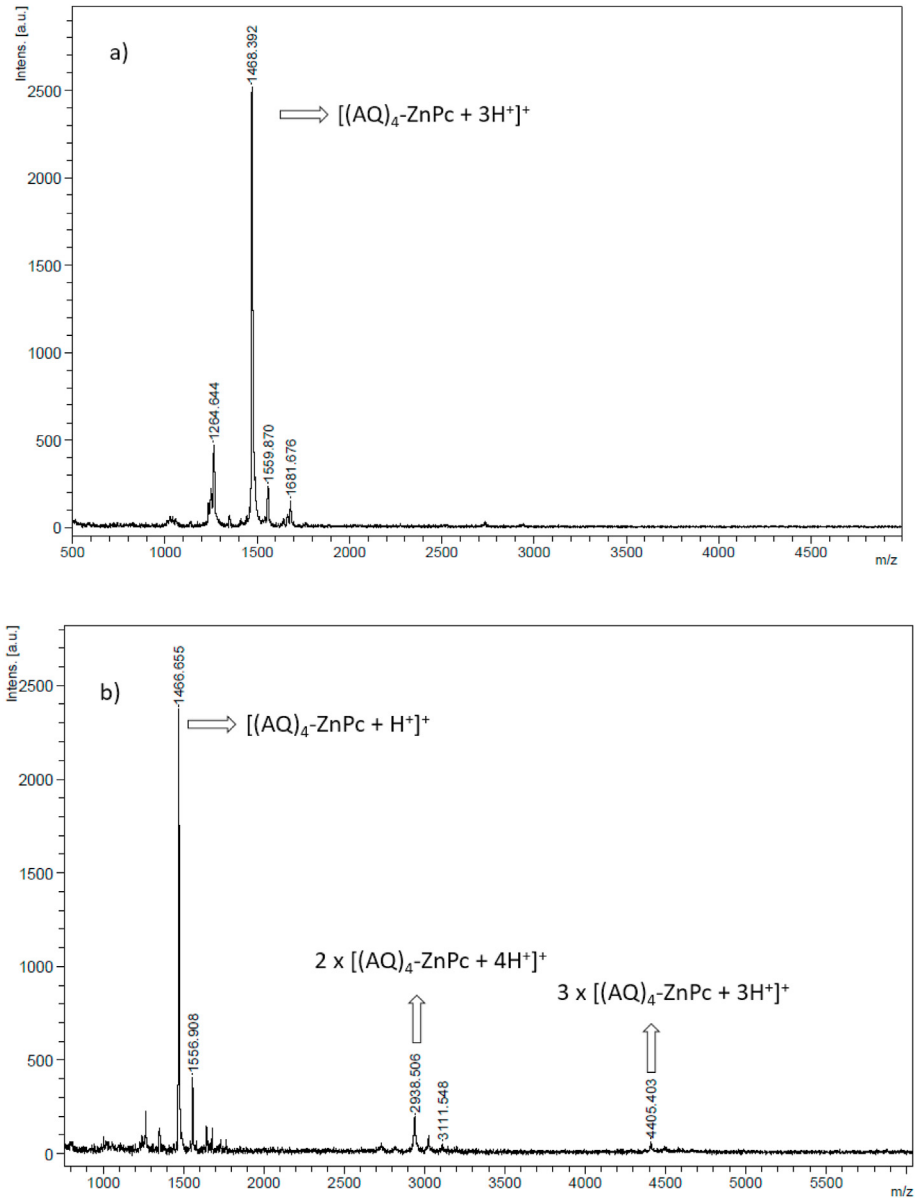

Fig. 3. The MALDI-TOF spectra of a) **$(AQ)_4$-ZnPc** in dry THF b) **$(AQ)_4$-ZnPc** in THF containing 15% water (the experiment was performed without matrix).

phenomenon. Besides, aniline and phenol have slightly decreasing effect of emission due to their polarity of amine and hydroxyl group character. However, the quenching of emission was slightly occurred by furan. On the other hand, DMF and DMSO are the two solvents that have axial coordination ability to the metal center of phthalocyanines [41]. We know from our previously published works that this ligand ability can differ depending on the metal and substituents of the phthalocyanine in the aspect of solubility and other intermolecular interactions [11,25]. For our probe molecule, considering the anthraquinone moiety and zinc metal, DMF is coordinated into zinc metal from axial position but this case was not formed for DMSO as observed for other zinc phthalocyanines in our previous studies. Because the UV–Vis spectrum of the **$(AQ)_4$-ZnPc** in DMSO exhibits very strong aggregation band compared to DMF solvent, which may prevent axial coordination of DMSO to zinc metal center of the phthalocyanine probe.

3.3. Quantification and detection limits

The spectral responses of **$(AQ)_4$-ZnPc** probe were examined by titrating with water in THF. The emission wavelength was recorded at 683 nm when the excitation wavelength was applied at 605 nm. Fig. 5a shows fluorescence intensity changes *vs.* increasing amount of water in THF. Fig. 5b displays the titration curve in the range of 0–4.84 $\times$ 10^{-2} M (0–980 ppm) water. The titration values of the sensor were fitted x- and y-axis, indicating molar concentration of water and intensity, respectively (Fig. 5b). Related quantification equation was given below.

Quantification Equation: $y = -3047.14x + 899.23$ ($R^2 = 0.997$) (1)

Moreover, Limit of Detection (LOD = 3α/Slope) was measured as 2.27 $\times$ 10^{-4} M (4.6 ppm) for seven parallel determination of blank

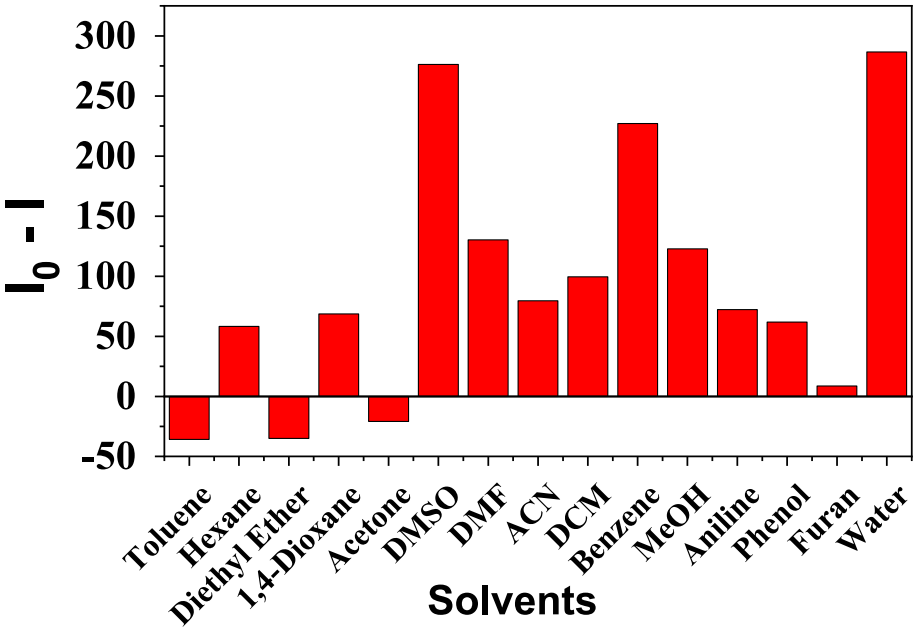

Fig. 4. The effect of the solvents (20 μl added) on the intensity of the emission of 9.0×10^{-6} M **$(AQ)_4$-ZnPc** in THF.

solution. This detection limit value is significantly low when compared to the previous studies in Table S1.

3.4. Stern-Volmer relationship

The mechanism of fluorescence quenching can be occurred as static or dynamic. The static quenching is normally connected with complexation between the ground-state of fluorophore and the quencher while the dynamic quenching arises from interaction between the quencher molecule and fluorophore at the short-lived excited state [43].

The fluorescence quenching of sensor **$(AQ)_4$-ZnPc** can be explained by Stern-Volmer equation in the presence of water.

$$I_0\backslash I = 1 + K_{sv}[Q] \quad (2)$$

Where I_0 is the emission intensity of the fluorescence in absence of water, I is the emission intensity in the presence of water, K_{sv} is the quenching constant and [Q] is the concentration of the quencher. The linear behavior of the plot of Stern-Volmer indicates that a dynamic quenching mechanism takes place between fluorophore and water molecules (Fig. 6a). The quenching constant K_{sv} that equals to the slope of the graph was calculated to measure the sensitivity of the sensor against to water molecules in THF, and found as 3.95 M^{-1}. This value is about two times higher than N-heteroaryl-1,8-naphthalimide fluorescent sensor that designed by Zhang et al. [9].

The response time of the sensor against water in THF was measured by taking continuously spectrum using automated mode of the device at near of the 683 nm during 140 s and the response time found as 1 s (Fig. 6b), which is the best value within the known fluorometric water sensors.

Table S1 illustrates the previous and our studies that were performed for trace amount of water detection in THF along with their LOD values and response mechanisms. As an example, a N-heteroaryl-1,8-naphthalimide derivate organic dye that is sensitive to solvent polarity was designed to track water in organic solvents. The probe molecule that works via ICT mechanism can detect water with 0.020%(wt) LOD in THF solvent [9]. A diketopyrrolopyrrole-based probe (DPP1) that has two characteristic response mechanisms ESIPT and AIE was synthesized to detect water in organic solvents. When the probe was reacted with fluoride anion to obtain (DPP1-F), the resulting system detects the water for 5 s with 0.0072% (wt) LOD in THF solvent [44]. A hydroxyl-containing polyimide based film that activated with fluoride anion to detect water was fabricated. The probe that works colorimetric and ratiometric can detects water for 3 s with 0.0015% (wt) LOD in DMF solvent [45]. Our study of fluorometric method, the linear range, limit of detection (LOD), and response time of sensor **$(AQ)_4$-ZnPc** were measured as 0–0.245 M, 0.00046 %wt LOD, and 1 s, respectively. By the study of voltammetric method, the linear range, LOD, and response time of **$(AQ)_4$-ZnPc** were measured as 0–1.64 M, 1.07×10^{-6} (%wt), and 1 min, respectively. To the best of our knowledge, sensor **$(AQ)_4$-ZnPc** is one of the most promising probe for water detection from the points of view such as response time, limit of detection and well-known chemical class of probe molecule.

3.5. Real sample experiment in three different THF solvents

To display the effectiveness and applicability of the probe, three real sample analysis were conducted showing the RSD and recovery value. First of all, the water content of three different THF solvent were measured using Karl-Fisher titration. After that, three different **$(AQ)_4$-ZnPc** probe solutions were prepared using the THF solvents in 7 ml test tubes as indicated in the measurement procedure. Table 1 illustrates the RSD and recovery values of the probe for 25, 505, and 895 ppm water content at which corresponds the beginning, middle, and final points of the calibration curve. Obtained values reveal that the sensor can be effectively applied as a sensor for water content measurement in THF solvents.

3.6. Quantification of water content in DMF by square wave voltammetry (SWV)

In this part of study, the sensor property of **$(AQ)_4$-ZnPc** was studied by SWV to quantify water content in DMF. First, electrochemistry of **$(AQ)_4$-ZnPc** and 9,10-anthraquinone **(AQ)** was

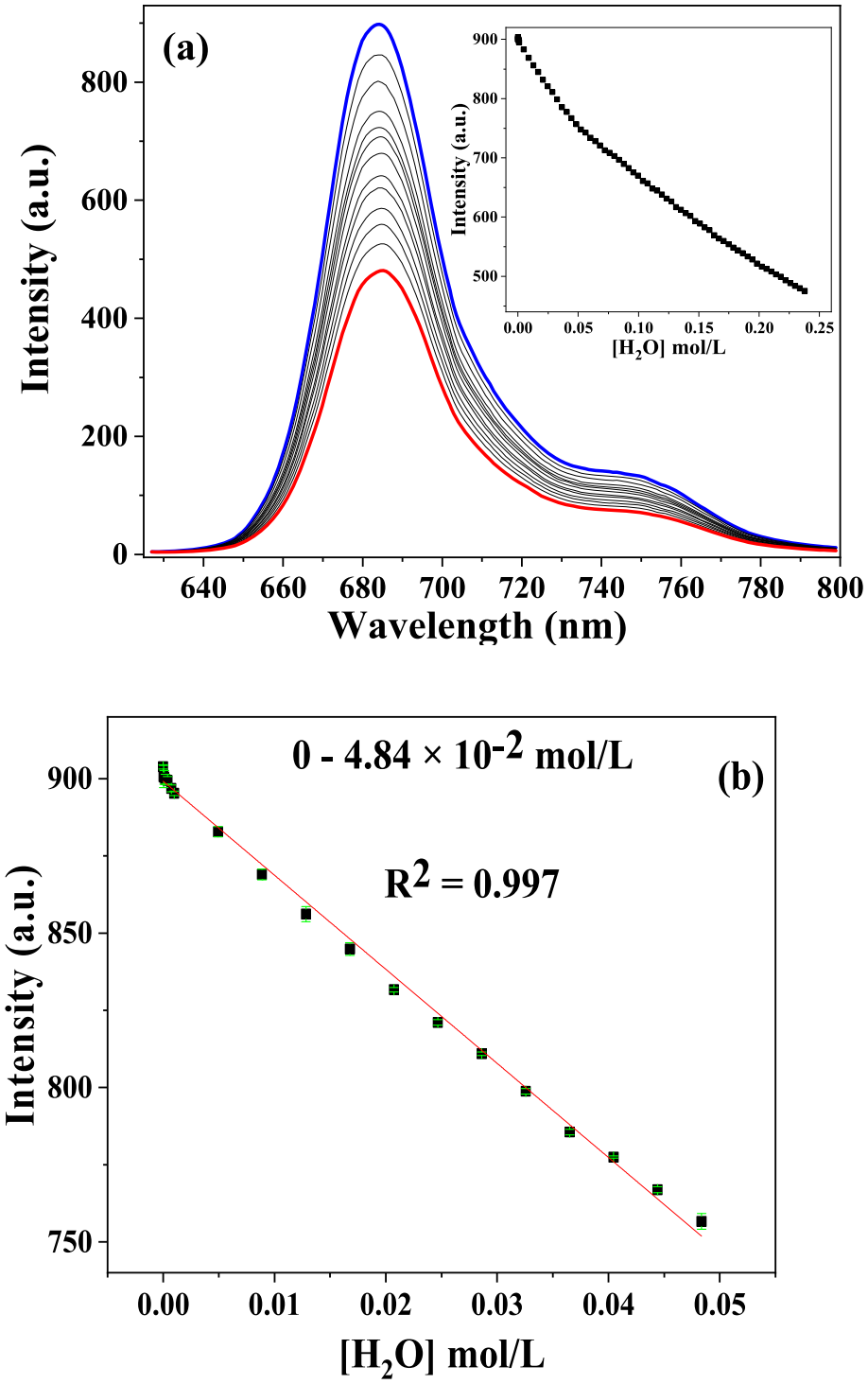

Fig. 5. (a) Fluorescence spectral changes of **$(AQ)_4$-ZnPc** (9.0×10^{-6} M) depending on addition of increasing amount of water in THF 0–0.245 M (0–4980 ppm water), (b) linear calibration graph for 0–4.84×10^{-2} M (0–980 ppm) water.

comparatively studied by the CV in the identical experimental condition in order to elucidate redox mechanism of **$(AQ)_4$-ZnPc**. As expected, **AQ** exhibits reversible one-electron reduction wave, producing monoanion (semiquinone radical, $AQ^{\bullet -}$). The half-wave potential of this process ($E^{(1)}{}_{1/2}$) was observed at −0.82 V with 0.11 V of the peak separation between anodic and cathodic peaks (ΔE_p) and 0.90 of the ratio of the anodic peak to cathodic peak (I_{pa}/I_{pc}). The further reversible reduction process with one-electron is evolved at more negative side at −1.49 V of V $E^{(2)}{}_{1/2}$ with 0.10 V of ΔE_p and 0.91 of I_{pa}/I_{pc} to generate dianion (the second reduction product, AQ^{2-}) by 0.100 V. s^{-1} scan rate (Fig. 7a). On the other hand, **[$(AQ)_4$-ZnPc]** displayed three reversible reduction and two oxidation processes in the presence of Ag/AgCl electrode. The oxidation processes are arising from the Pc macrocycle because the **AQ** unit and zinc metal into the cavity of the Pc ring do not exhibit an electro-oxidation process. The first and second oxidation processes

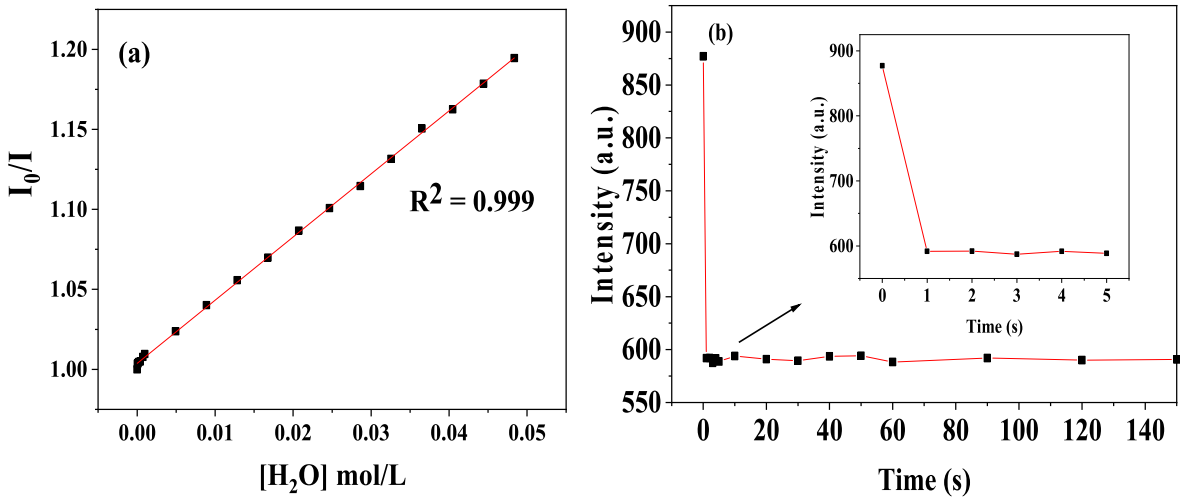

Fig. 6. (a) Stern-Volmer graph of I_0/I *vs.* $[H_2O]$ in THF, (b) the response time of the sensor against water (15 μL) in THF.

Table 1
Real sample results for determination of water in THF samples.

Sensor	Added (M)	Recovery (%)	RSD
$(AQ)_4$-ZnPc	0.0012 (25 ppm)	97	5
	0.02491 (505 ppm)	98	0.4
	0.04391 (895 ppm)	99	1.7

are represented as the redox couple **$(AQ)_4$-ZnPc/$(AQ)_4$-ZnPc$^+$** and **$(AQ)_4$-ZnPc/$(AQ)_4$-ZnPc^{2+}** in Scheme 1. The $E^{(ox1)}{}_{1/2}$ and $E^{(ox2)}{}_{1/2}$ of these processes were calculated as 0.57 V with 0.06 V of ΔE_p and 0.96 of I_{pc}/I_{pa}, and 0.85 V with 0.07 V of ΔE_p and 0.86 of I_{pa}/I_{pc}, respectively. Also, reduction waves corresponding to the four anthraquinone units attached to **[$(AQ)_4$-ZnPc]** dominate the reduction side of **$(AQ)_4$-ZnPc**. When the CVs of the **AQ** and **$(AQ)_4$-ZnPc** were compared it was obviously seen that the first and third reduction processes of **$(AQ)_4$-ZnPc** belong to singly reduced **($AQ^{\bullet-}$)** and doubly reduced **(AQ^{2-})** four anthraquinone units on **$(AQ)_4$-ZnPc** molecule, represented as **$(AQ^{\bullet-})_4$-ZnPc** and **$(AQ)_4^{2-}$-ZnPc$^-$** in Scheme 1, which displayed at −0.77 V of $E^{(red1)}{}_{1/2}$ with 0.072 V of ΔE_p and 0.90 of I_{pa}/I_{pc}, and −1.39 V of $E^{(red3)}{}_{1/2}$ with 0.13 V of ΔE_p and 0.92 of I_{pa}/I_{pc}, respectively. These reduction potentials are not significantly affected relative to those of **AQ** molecule. The second reduction wave observed at −0.99 V of $E^{(red2)}{}_{1/2}$ with 0.06 V of ΔE_p and 0.90 of I_{pa}/I_{pc} is based on the Pc ring (**$(AQ^{\bullet-})_4$-ZnPc/$(AQ^{\bullet-})_4$-ZnPc$^-$**), which has a lower current density than those of the reduction processes of **AQ**. The difference between $E^{(ox1)}{}_{1/2}$ and $E^{(red2)}{}_{1/2}$ corresponding to the Pc ring (1.52 V) is consistent with those to ZnPcs [11]. Interestingly, we could not observe further reduction processes related with the Pc ring, probably due to highly negatively charged of **$(AQ)_4$-ZnPc** molecule.

When the voltammogram belonging to **$(AQ)_4$-ZnPc** is examined to elucidate the electron transfer mechanism, it is understood that the current of the anodic peak corresponding to the third reduction wave is smaller than that of the first reduction wave (Fig. 7b). The current loss is likely due to the complexation of the neutral form of **$(AQ)_4$-ZnPc** with the third-reduced product **$(AQ^{2-})_4$-ZnPc$^-$** or the adsorption of the third reduced products to the surface of the electrode. Our previous study on the ferrocene-derived naphthoquinone supports this situation [28]. Scheme 1 represents the mechanism of the electron transfer reaction of **$(AQ)_4$-ZnPc** in the absence and presence of water in DMF in the electrochemical cell. In Scheme 1, the reversible interactions between sensor **$(AQ)_4$-ZnPc** and water molecules are illustrated through the anion radical and polyanion type of each anthraquinone unit of the Pc.

Fig. 8a shows the SWV of **$(AQ)_4$-ZnPc** where water is sequentially added into DMF. Blue line belongs to the SWV of **$(AQ)_4$-ZnPc** at 1.65 M water in DMF. Depending on increasing amount of water, the first and third reduction potentials ($E^{(red1)}$ and $E^{(red3)}$, respectively) corresponding to **($AQ^{\bullet-}$)$_4$-ZnPc** and **$(AQ^{2-})_4$-ZnPc$^-$** species shifted to more positive region. However, the first oxidation and second reduction potentials ($E^{(ox1)}$ and $E^{(red2)}$, respectively) belonging to the Pc ring **$(AQ)_4$-ZnPc$^+$** and **($AQ^{\bullet-}$)$_4$-ZnPc$^-$**) maintained their potential values even at high water concentration. The

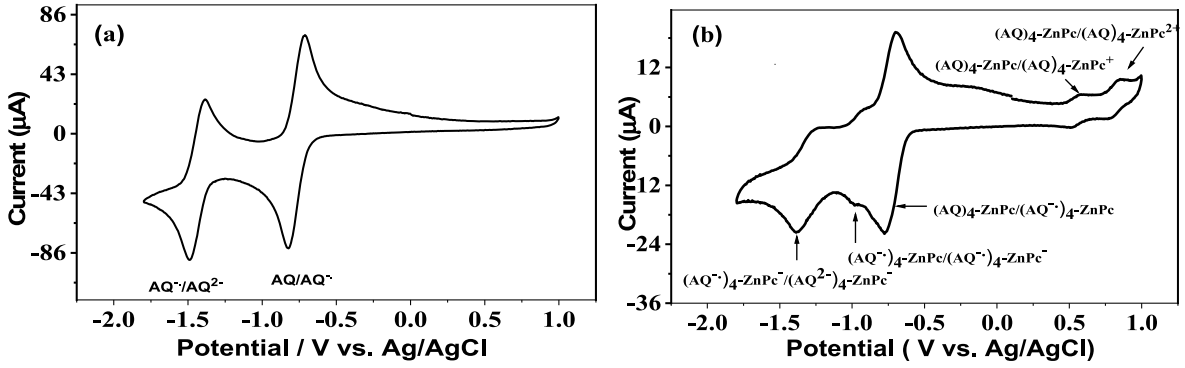

Fig. 7. (a) The CVs of **AQ** and (b) **$(AQ)_4$-ZnPc** in DMF solution with 0.1 M TBAP. W.E: GCE with 3.0 mm diameter and scan rate: 0.100 V. s^{-1} scan rate.

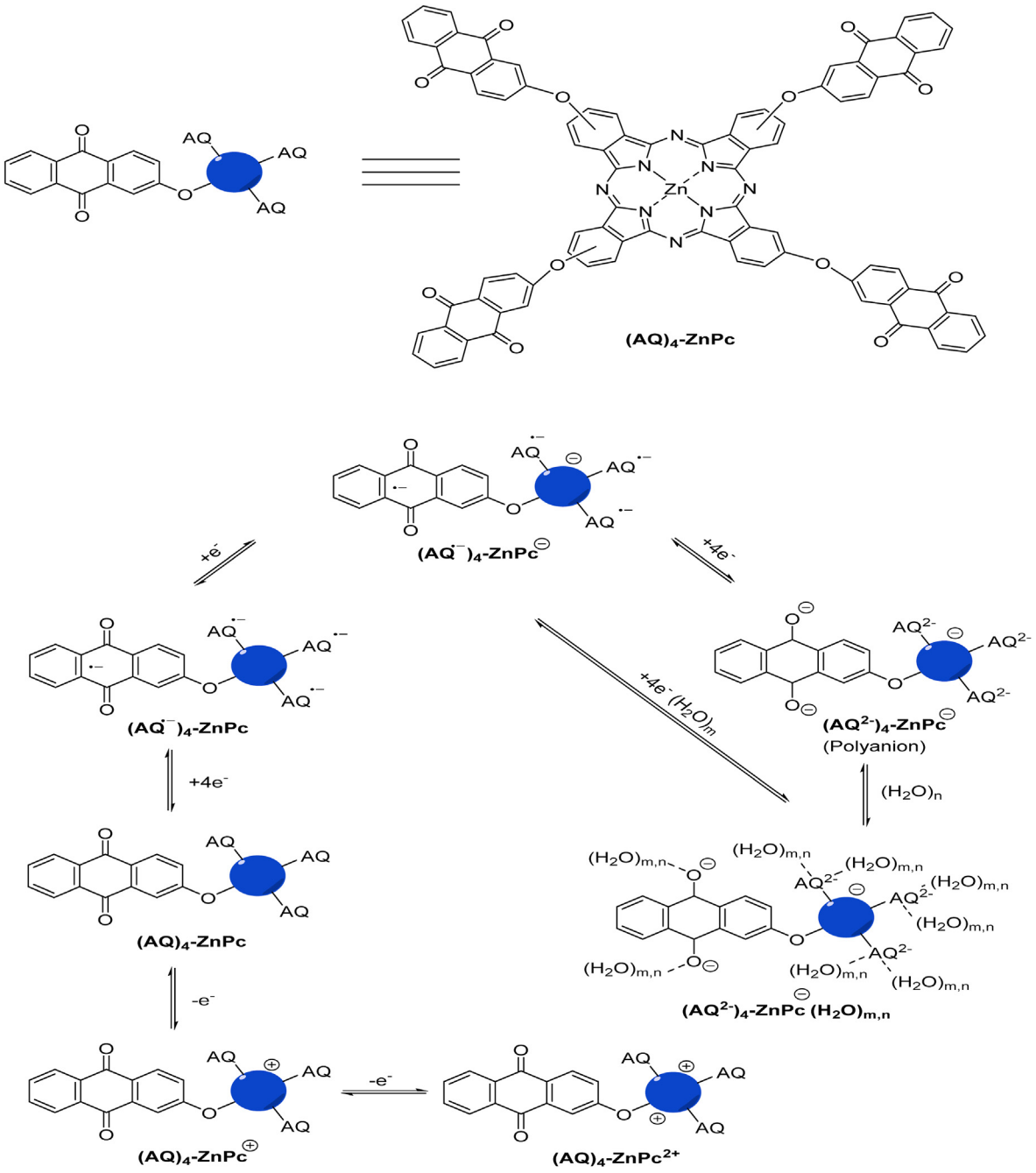

Scheme 1. The mechanism of the electron transfer reaction of **(AQ)$_4$-ZnPc** in the absence and presence of water in the electrochemical cell.

shift observed for the reduction of **AQ** units on the Pc ring was attributed to the stabilization of the reduction products **(AQ$^{\bullet-}$)$_4$-ZnPc** and **(AQ^{2-})$_4$-ZnPc$^-$** via the hydrogen bonding formed with the interaction of the reduced products and water in DMF as described for some quinone and naphthoquinone reduced species by different research groups [26,46–49].

The third reduction potential ($E^{(red3)}$) was more shifted to positive side (0.24 V) than the first reduction potential $E^{(red1)}$ (0.0189 V) for the same quantity of water (1.65 M) in DMF because the further reduced anthraquinone moieties on the Pc ring which have extremely negative charge on the carbonyl oxygen effectively favor the formation of the hydrogen bonding with water. The first oxidation and second reduction potentials ($E^{(ox1)}$ and $E^{(red2)}$) based on the Pc macrocycle display no potential change as the concentration of water increases. In the approach of the voltammetric method based on the potential shift, this critical property of the Pc was utilized as an internal standard to accurately determine of water content in DMF.

To investigate the electrochemical behavior of the **(AQ)$_4$-ZnPc** in different organic contaminants/solvents, additional experiments were performed by adding 15 μl of these solvents in **(AQ)$_4$-ZnPc** probe DMF solution. While the highest potential shift was observed by adding water, alcoholic solvents like EtOH and MeOH were caused similar shifting effect on the second reduction peak (Figs. S7 and S8). The results are consistent with the proposed electrochemical sensing mechanism with water via hydrogen bonding

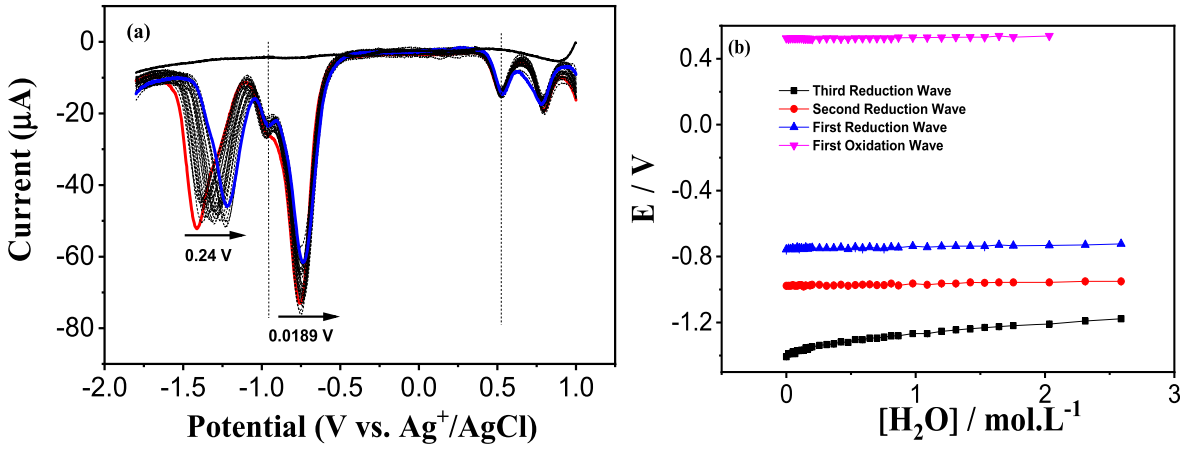

Fig. 8. (a) The SWV changes of **(AQ)$_4$-ZnPc** in DMF solution with 0.2 M TBAP. Red line: no water in DMF; dash black line: step by step water addition into DMF. Blue solid line: the final water addition into DMF (1.65 M); solid black line: the background SWV of the solution without the sensor. The concentration of **(AQ)$_4$-ZnPc** = 2.0×10^{-3} M, W.E: GCE with 3.0 mm diameter. Step Height: 2.00 mV; Pulse PH/PW: 0.025 V for 0.01 s; Scan rate: 0.100 V s^{-1}, (b) the plots corresponding to the $E_{1/2}$ of the first oxidation (pink triangle), the first reduction (blue triangle), second reduction (red circle), and the third reduction (black square), waves *vs.* concentration of water in DMF. (For interpretation of the references to color in this figure legend, the reader is referred to the Web version of this article.)

interaction between carbonyl group of anthraquinone and alcohols. Even though other solvents have no significant effect on the second reduction peak, DMSO shifts the second reduction peak as 30 mV.

The plots of the cathodic peak potentials for the first oxidation, first reduction, and third reduction waves *vs.* increasing water concentration in DMF are represented in Fig. 8b where it is seen that the $E^{(red3)}$ values shifts to anodic side with step by step addition of water into DMF, but the $E^{(ox1)}$ and $E^{(red2)}$ values play no potential changes in the identical experimental condition. It is concluded that the hydrogen bonding formed with the interaction of the water molecules and reduced products **(AQ$^{\cdot-}$)$_4$-ZnPc** and **(AQ^{2-})$_4$-ZnPc$^-$** is the redox-dependent interactions (Scheme 1). The equilibrium constants ($K^{(1)}$ and $K^{(2)}$) and the average number of the binding water molecules (*n* and *m*) related with the monoanion radicals and polyanion products are calculated via equations **(9)** and **(12)** for the first and third reduction processes (in Supporting Information, calculations in electrochemical sensing).

Thus, in Fig. S9b, the graph of $E^{(red3)}_{1/2}$ *vs.* log[H_2O] can be drawn. Its slope is equal to 2.303 (*m*-*n*) RT/4F, and *m* value were calculated as 10.4 and $K^{(2)}$ value is equal to the intercept of the graph and its value has been found as 1.6×10^{11} $M^{-(m-n)}$.

The above-mentioned internal standard concept was applied here for the first oxidation and reduction potentials of the Pc molecule. It is understood that ($E^{(red2)}_{1/2}$ -$E^{(red3)}_{1/2}$) and ($E^{(ox1)}_{1/2}$ - $E^{(red3)}_{1/2}$) could be applied for accurately determine water content in DMF. Fig. 9 shows the calibration plots of ($E^{(red2)}_{1/2}$ - $E^{(red3)}_{1/2}$) *vs.* log[H_2O] and ($E^{(ox1)}_{1/2}$ - $E^{(red3)}_{1/2}$) *vs.* log [H_2O].

From the graphs shown in Fig. 9a and b, the linear calibration lines with $R^2 = 0.984$ and $R^2 = 0.985$, respectively were obtained. Thus, one can enable an accurate determination of water content in DMF with a LOD value (LOD = 3α/Slope) of 6.02×10^{-7} M over the calibrated values ($E^{(red2)}_{1/2}$ - $E^{(red3)}_{1/2}$) or with a LOD value of 5.64×10^{-7} M over the calibrated values ($E^{(ox1)}_{1/2}$ - $E^{(red3)}_{1/2}$). Using sensor **(AQ)$_4$-ZnPc**, if a single SWV is recorded, the water content in DMF can be determined accurately with the calibration graphs without the need for an external calibrant molecule.

4. Conclusion

For many chemical reactions and electrochemical studies carried out in organic solvents, the presence of trace amounts of water is considered as impurity and reaction disruptive. Therefore,

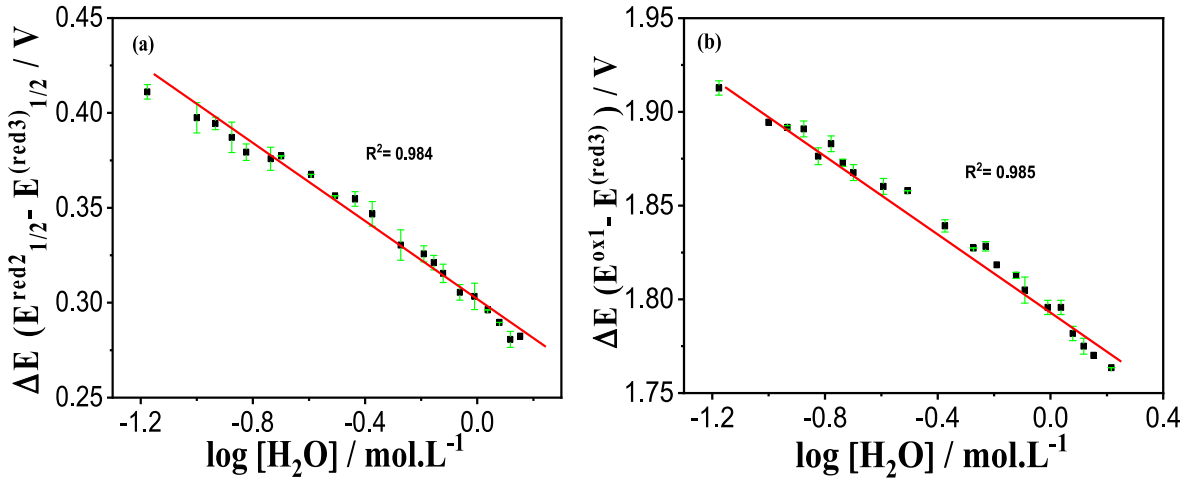

Fig. 9. (a) The calibration plots of ($E^{(red2)}_{1/2}$ - $E^{(red3)}_{1/2}$) *vs.* log[H_2O] and (b) ($E^{(ox1)}_{1/2}$ - $E^{(red3)}_{1/2}$) *vs.* log [H_2O]. (For interpretation of the references to color in this figure legend, the reader is referred to the Web version of this article.)

construction of new sensors with improved analytical performances such as low LOD, response time, and photochemical stability of fluorophore is needed to accurately quantification of water content in the solvent medium. Herein, a new sensor platform based on the anthraquinone functional zinc phthalocyanine **$(AQ)_4$-ZnPc** was utilized for quantification of water content in the solvents of THF and DMF. The sensor developed in this study has some important advantages; *i*. the sensor has photochemical stability during the experiments, *ii*. the sensor allows water determination to be conducted by both fluorometric and voltammetric methods, *iii*. the sensor has the shortest response time when compared to the sensors known in the literature for water determination, *iv*. the aggregation property of Pc molecules was applied for determination of water in THF, *v*. the redox chemistry of the Pc ring was first time used as a calibrant for water quantitation in DMF. In summary, the combination of anthraquinone and phthalocyanine molecules provided superior analytical performance in determining trace amounts of water in THF and DMF. The study will shed light on the design of new Pc compound combining with varying functional molecules with different properties for sensor or different applications.

CRediT authorship contribution statement

Mustafa Semih Yildirim: Methodology, Validation, Investigation, Writing – original draft. **Yusuf Alcay:** Methodology, Validation, Investigation. **Ozgur Yavuz:** Methodology, Validation, Investigation. **Secil Kirlangic Atasen:** Methodology, Validation, Investigation. **Zeliha Mermer:** Methodology, Validation, Investigation. **Hulya Aribuga:** Methodology, Validation, Investigation. **Ismail Yilmaz:** Conceptualization, Supervision, Writing – review & editing.

Declaration of competing interest

The authors declare that they have no known competing financial interests or personal relationships that could have appeared to influence the work reported in this paper.

Acknowledgements

We would like to thank Istanbul Technical University for support.

Appendix A. Supplementary data

Supplementary data to this article can be found online at https://doi.org/10.1016/j.aca.2022.339531.

References

[1] X.Y. Wang, C.G. Niu, L.Y. Hu, D.W. Huang, S.Q. Wu, L. Zhang, X.J. Wen, G.M. Zeng, A fluorescent ratiometric sensor based on covalent immobilization of chalcone derivative and porphyrin Zinc for detecting water content in organic solvents, Sensor. Actuator. B Chem. 243 (2017) 1046–1056, https://doi.org/10.1016/j.snb.2016.12.084.

[2] Q. Xue, X. Tang, Y. Li, H. Liu, X. Duan, Contactless and simultaneous measurement of water and acid contaminations in oil using a flexible microstrip sensor, ACS Sens. 5 (2020) 171–179, https://doi.org/10.1021/acssensors.9b01965.

[3] U. Fegade, S. Patil, R. Kaur, S.K. Sahoo, N. Singh, R. Bendre, A. Kuwar, A novel chromogenic and fluorogenic chemosensor for detection of trace water in methanol, Sensor. Actuator. B Chem. 210 (2015) 324–327, https://doi.org/10.1016/j.snb.2014.12.126.

[4] C. Pinheiro, J.C. Lima, A.J. Parola, Using hydrogen bonding-specific interactions to detect water in aprotic solvents at concentrations below 50 ppm, Sensor. Actuator. B Chem. 114 (2006) 978–983, https://doi.org/10.1016/j.snb.2005.08.013.

[5] J. Blyth, R.B. Millington, A.G. Mayes, E.R. Frears, C.R. Lowe, Holographic sensor for water in solvents, Anal. Chem. 68 (1996) 1089–1094, https://doi.org/10.1021/ac9509115.

[6] S. Tomita, H. Tachino, N. Kasahara, Water sensor with optical fiber, J. Lightwave Technol. 8 (1990) 1829–1832, https://doi.org/10.1109/50.62878.

[7] A.E. Clough, Measuring the water content of synthetic lubricants with polymer-coated sensors, Anal. Chim. Acta 315 (1995) 15–26, https://doi.org/10.1016/0003-2670(95)00304-I.

[8] Q. Deng, Y. Li, J. Wu, Y. Liu, G. Fang, S. Wang, Y. Zhang, Highly sensitive fluorescent sensing for water based on poly(m-aminobenzoic acid), Chem. Commun. 48 (2012) 3009–3011, https://doi.org/10.1039/c2cc17856g.

[9] Z. Li, Q. Yang, R. Chang, G. Ma, M. Chen, W. Zhang, N-Heteroaryl-1,8-naphthalimide fluorescent sensor for water: molecular design, synthesis and properties, Dye, Pigment 88 (2011) 307–314, https://doi.org/10.1016/j.dyepig.2010.07.009.

[10] S. Song, Y. Zhang, Y. Yang, C. Wang, Y. Zhou, C. Zhang, Y. Zhao, M. Yang, Q. Lin, Ratiometric fluorescence detection of trace water in organic solvents based on aggregation-induced emission enhanced Cu nanoclusters, Analyst 143 (2018) 3068–3074, https://doi.org/10.1039/c8an00450a.

[11] O. Yavuz, Y. Alcay, K. Kaya, M. Sezen, S. Kirlangic Atasen, M.S. Yildirim, Y. Ozkilic, N.Ş. Tuzun, I. Yilmaz, Superior sensor for Be^{2+} ion recognition via the unprecedented octahedral crystal structure of a one-dimensional coordination polymer of crown fused zinc phthalocyanine, Inorg. Chem. 58 (2019) 909–923, https://doi.org/10.1021/acs.inorgchem.8b03038.

[12] Z.M. Dang, Y. Gao, H.P. Xu, J. Bai, Fabrication and characteristics of organic semiconductor nanoparticles of copper phthalocyanine oligomers, J. Colloid Interface Sci. 322 (2008) 491–496, https://doi.org/10.1016/j.jcis.2008.03.012.

[13] O.L. Kaliya, E.A. Lukyanets, G.N. Vorozhtsov, Catalysis and photocatalysis by phthalocyanines for technology, ecology and medicine, J. Porphyr. Phthalocyanines 3 (1999) 592–610, https://doi.org/10.1002/(SICI)1099-1409(199908/10)3:6/7<592::AID-JPP180>3.0.CO;2-G.

[14] H. Ali, J.E. van Lier, Metal complexes as photo- and radiosensitizers, Chem. Rev. 99 (1999) 2379–2450, https://doi.org/10.1021/cr980439y.

[15] O.J. Achadu, T. Nyokong, Graphene quantum dots anchored onto mercaptopyridine-substituted zinc phthalocyanine-Au@Ag nanoparticle hybrid: application as fluorescence "off-on-off" sensor for Hg^{2+} and biothiols, Dyes Pigments 145 (2017) 189–201, https://doi.org/10.1016/j.dyepig.2017.06.002.

[16] S. Ouedraogo, S. Ouedraogo, R. Meunier-Prest, A. Kumar, M. Bayo-Bangoura, M. Bouvet, Modulating the electrical properties of organic heterojunction devices based on phthalocyanines for ambipolar sensors, ACS Sens. 5 (2020) 1849–1857, https://doi.org/10.1021/acssensors.0c00877.

[17] T.V. Basova, C. Taşaltin, A.G. Gürek, M.A. Ebeoğlu, Z.Z. Öztürk, V. Ahsen, Mesomorphic phthalocyanine as chemically sensitive coatings for chemical sensors, Sensor. Actuator. B Chem. 96 (2003) 70–75, https://doi.org/10.1016/S0925-4005(03)00487-8.

[18] D. Wöhrle, V. Schmidt, Octabutoxyphthalocyanine, a new electron donor, J. Chem. Soc., Dalton Trans. (1988) 549–551, https://doi.org/10.1039/DT9880000549.

[19] P.D. Hale, W.J. Pietro, M.A. Ratner, D.E. Ellis, T.J. Marks, On the electronic structure of substituted phthalocyanines: a Hartree-Fock-slater study of octacyano- and octafluoro-substituted (Phthalocyaninato)silicon dihydroxide, J. Am. Chem. Soc. 109 (1987) 5943–5947, https://doi.org/10.1021/ja00254a007.

[20] H. Matsuzaki, T.N. Murakami, N. Masaki, A. Furube, M. Kimura, S. Mori, Dye aggregation effect on interfacial electron-transfer dynamics in zinc phthalocyanine-sensitized solar cells, J. Phys. Chem. C 118 (2014) 17205–17212, https://doi.org/10.1021/jp500798c.

[21] X.F. Zhang, H.J. Xu, Influence of halogenation and aggregation on photosensitizing properties of zinc phthalocyanine (ZnPC), J. Chem. Soc., Faraday Trans. 89 (1993) 3347–3351, https://doi.org/10.1039/FT9938903347.

[22] I. Yilmaz, S. Arslan, S. Guney, I. Becerik, Synthesis, electrospectroelectrochemical characterization and electrocatalytic behavior towards dioxygen reduction of a new water-soluble cobalt phthalocyanine containing naphthoxy-4-sulfonic acid sodium salt, Electrochim. Acta 52 (2007) 6611–6621, https://doi.org/10.1016/j.electacta.2007.04.055.

[23] S. Wang, F. Li, Y. Wang, D. Qiao, C. Sun, J. Liu, A superior oxygen reduction reaction electrocatalyst based on reduced graphene oxide and iron(II) phthalocyanine-supported sub-2 nm platinum nanoparticles, ACS Appl. Nano Mater. 1 (2018) 711–721, https://doi.org/10.1021/acsanm.7b00173.

[24] D. Zhang, M. Zhu, L. Zhao, J. Zhang, K. Wang, D. Qi, Y. Zhou, Y. Bian, J. Jiang, Ratiometric fluorescent detection of Pb2+ by FRET-based phthalocyanine-porphyrin dyads, Inorg. Chem. 56 (2017) 14533–14539, https://doi.org/10.1021/acs.inorgchem.7b02261.

[25] O. Yavuz, M. Sezen, Y. Alcay, M.S. Yildirim, K. Kaya, Y. Ozkilic, N.Ş. Tuzun, I. Yilmaz, A new perspective on the beryllium sensor platform: low symmetry phthalocyanine-based molecular design and ultra trace amount Be^{2+} ion recognition in aqueous media, Sensor. Actuator. B Chem. 329 (2021), https://doi.org/10.1016/j.snb.2020.129002, 129002.

[26] N. Gupta, H. Linschitz, Hydrogen-bonding and protonation effects in electrochemistry of quinones in aprotic solvents, J. Am. Chem. Soc. 119 (1997) 6384–6391, https://doi.org/10.1021/ja970028j.

[27] S.H. Kim, H.S. Choi, J. Kim, S.J. Lee, D.T. Quango, J.S. Kim, Novel optical/electrochemical selective 1,2,3-triazole ring-appended chemosensor for the Al^{3+}

ion, Org. Lett. 12 (2010) 560–563, https://doi.org/10.1021/ol902743s.
[28] M. Dagdevren, I. Yilmaz, B. Yucel, M. Emirik, A novel ferrocenyl naphthoquinone fused crown ether as a multisensor for water determination in acetonitrile and selective cation binding, J. Phys. Chem. B 119 (2015) 12464–12479, https://doi.org/10.1021/acs.jpcb.5b06590.
[29] Y.H. Kim, M.G. Choi, H.G. Im, S. Ahn, I.W. Shim, S.K. Chang, Chromogenic signalling of water content in organic solvents by hydrazone-acetate complexes, Dyes Pigments 92 (2012) 1199–1203, https://doi.org/10.1016/j.dyepig.2011.07.019.
[30] P. Kumar, R. Sakla, A. Ghosh, D.A. Jose, Reversible colorimetric sensor for moisture detection in organic solvents and application in inkless writing, ACS Appl. Mater. Interfaces 9 (2017) 25600–25605, https://doi.org/10.1021/acsami.7b05335.
[31] H.S. Jung, P. Verwilst, W.Y. Kim, J.S. Kim, Fluorescent and colorimetric sensors for the detection of humidity or water content, Chem. Soc. Rev. 45 (2016) 1242–1256, https://doi.org/10.1039/c5cs00494b.
[32] M.S. Kahouech, K. Hriz, S. Touaiti, J. Bassem, New anthracene-based-phtalocyanine semi-conducting materials: synthesis and optoelectronic properties, Mater. Res. Bull. 75 (2016) 144–154, https://doi.org/10.1016/j.materresbull.2015.11.010.
[33] S. Arslan, I. Yilmaz, A new water-soluble metal-free phthalocyanine substituted with naphthoxy-4-sulfonic acid sodium salt. Synthesis, aggregation, electrochemistry and in situ spectroelectrochemistry, Polyhedron 26 (2007) 2387–2394, https://doi.org/10.1016/j.poly.2006.11.047.
[34] L. Breloy, V. Brezová, A. Blacha-Grzechnik, M. Presset, M.S. Yildirim, I. Yilmaz, Y. Yagci, D.L. Versace, Visible light anthraquinone functional phthalocyanine photoinitiator for free-radical and cationic polymerizations, Macromolecules 53 (2020) 112–124, https://doi.org/10.1021/acs.macromol.9b01630.
[35] D.B.G. Williams, M. Lawton, Drying of organic solvents: quantitative evaluation of the efficiency of several desiccants, J. Org. Chem. 75 (2010) 8351–8354, https://doi.org/10.1021/jo101589h.
[36] A. Ogunsipe, J.-Y. Chen, T. Nyokong, Photophysical and photochemical studies of zinc(II) phthalocyanine derivatives-effects of substituents and solvents, (n.d.). https://doi.org/10.1039/b315319c.
[37] N. Akkaya, A.T. Bilgiçli, A. Aytekin, M.N. Yarasir, M. Kandaz, Novel metal(III) and metal free soft phthalocyanine metal ion sensors bearing (1-hydroxyhexan-3-ylthio)-substituents: synthesis, characterization, aggregation behavior, Polyhedron 85 (2015) 857–863, https://doi.org/10.1016/j.poly.2014.10.014.
[38] E.T. Saka, M. Durmuş, H. Kantekin, Solvent and central metal effects on the photophysical and photochemical properties of 4-benzyloxybenzoxy substituted phthalocyanines, J. Organomet. Chem. 696 (2011) 913–924, https://doi.org/10.1016/j.jorganchem.2010.10.024.
[39] M.A. Rauf, S. Hisaindee, J.P. Graham, M. Nawaz, Solvent effects on the absorption and fluorescence spectra of Cu(II)-phthalocyanine and DFT calculations, J. Mol. Liq. 168 (2012) 102–109, https://doi.org/10.1016/j.molliq.2012.01.008.
[40] A. Ogunsipe, D. Maree, T. Nyokong, Solvent effects on the photochemical and fluorescence properties of zinc phthalocyanine derivatives, J. Mol. Struct. 650 (2003) 131–140, https://doi.org/10.1016/S0022-2860(03)00155-8.
[41] A. Ogunsipe, T. Nyokong, Effects of substituents and solvents on the photochemical properties of zinc phthalocyanine complexes and their protonated derivatives, J. Mol. Struct. 689 (2004) 89–97, https://doi.org/10.1016/j.molstruc.2003.10.024.
[42] T. Qiu, X. Xu, X. Qian, Solvent effects for fluorescence and absorption of tetra (fluoroalkyl) metallophthalocyanines: fluorocarbon solvent cage, J. Photochem. Photobiol. A Chem. 214 (2010) 86–91, https://doi.org/10.1016/j.jphotochem.2010.06.012.
[43] S. Mukhopadhyay, R.K. Gupta, R.P. Paitandi, N.K. Rana, G. Sharma, B. Koch, L.K. Rana, M.S. Hundal, D.S. Pandey, Synthesis, structure, DNA/protein binding, and anticancer activity of some half-sandwich cyclometalated Rh(III) and Ir(III) complexes, Organometallics 34 (2015) 4491–4506, https://doi.org/10.1021/acs.organomet.5b00475.
[44] F. Wu, L. Wang, H. Tang, D. Cao, Excited state intramolecular proton transfer plus aggregation-induced emission-based diketopyrrolopyrrole luminogen: photophysical properties and simultaneously discriminative detection of trace water in three organic solvents, Anal. Chem. 91 (2019) 5261–5269, https://doi.org/10.1021/acs.analchem.9b00032.
[45] Y. Wu, J. Ji, Y. Zhou, Z. Chen, S. Liu, J. Zhao, Ratiometric and colorimetric sensors for highly sensitive detection of water in organic solvents based on hydroxyl-containing polyimide-fluoride complexes, Anal. Chim. Acta 1108 (2020) 37–45, https://doi.org/10.1016/J.ACA.2020.02.043.
[46] Y. Hui, E.L.K. Chng, C.Y.L. Chng, H.L. Poh, R.D. Webster, Hydrogen-bonding interactions between water and the one- and two-electron-reduced forms of vitamin K 1 : applying quinone electrochemistry to determine the moisture content of non-aqueous solvents, J. Am. Chem. Soc. 131 (2009) 1523–1534, https://doi.org/10.1021/ja8080428.
[47] Y. Hui, E.L.K. Chng, L.P.-L. Chua, W.Z. Liu, R.D. Webster, Voltammetric method for determining the trace moisture content of organic solvents based on hydrogen-bonding interactions with quinones, Anal. Chem. 82 (2010), https://doi.org/10.1021/ac9026719, 1928–1934.
[48] E. Laviron, Electrochemical reactions with protonations at equilibrium. Part XIII. Experimental study of the homogeneous electron exchange in quinone/dihydroquinone systems, J. Electroanal. Chem. 208 (1986) 357–372, https://doi.org/10.1016/0022-0728(86)80543-5.
[49] M.W. Lehmann, D.H. Evans, Anomalous behavior in the two-step reduction of quinones in acetonitrile, J. Electroanal. Chem. 500 (2001) 12–20, https://doi.org/10.1016/S0022-0728(00)00234-5.